

Supporting Information

A First Principles Exploration on the Versatile Configurations at Alkynyl-protected Coinage Metal(111) Interface

Fang Sun and Qing Tang*

School of Chemistry and Chemical Engineering, Chongqing Key Laboratory of Theoretical and Computational Chemistry, Chongqing University, Chongqing 401331, China

*To whom correspondence should be addressed. E-mail: qingtang@cqu.edu.cn.

Table S1. Binding energies (BE: eV) and the optimized structures (only the topmost surface layer is shown) of methylethynyl ($\text{CH}_3\text{-C}\equiv\text{C-}$) at different adsorption sites on Au (111) with 4 layers of slab in a 4×4 lateral cell. The initial angle between the 111 plane and linear methylethynyl is 90° .

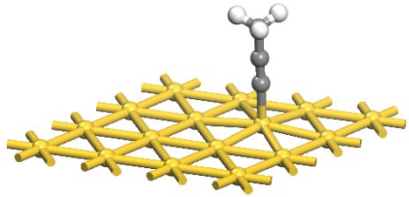
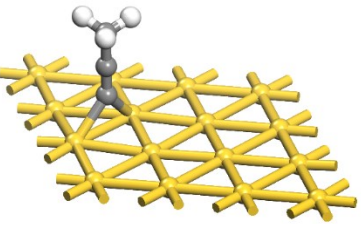
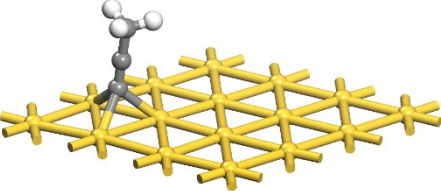
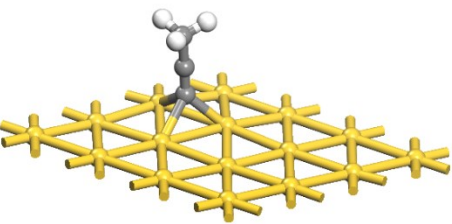
Sites	The optimized structures	BE (eV)
top		-3.06
bridge		-3.34
hcp		-3.40
fcc		<u>-3.45</u>

Table S2. Binding energies (BE: eV) and the optimized structures (only the topmost surface layer is shown) of methylethynyl ($\text{CH}_3\text{-C}\equiv\text{C-}$) at different adsorption sites on Ag (111) with 4 layers of slab in a 4×4 lateral cell. The initial angle between the 111 plane and linear methylethynyl is 90° .

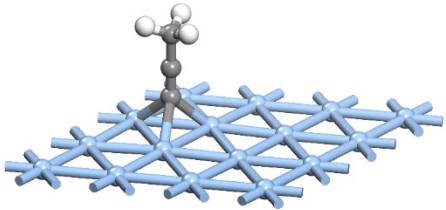
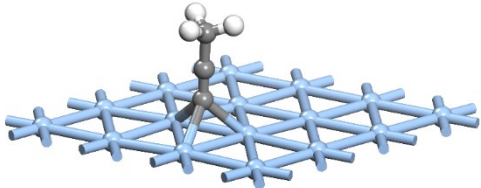
Sites	The optimized structures	BE (eV)
top	Relaxed to hcp	/
bridge	Relaxed to fcc	/
hcp		-3.54
fcc		<u>-3.55</u>

Table S3. Binding energies (BE: eV) and the optimized structures (only the topmost surface layer is shown) of methylethynyl ($\text{CH}_3\text{-C}\equiv\text{C-}$) at different adsorption sites on Cu (111) with 4 layers of slab in a 4×4 lateral cell. The initial angle between the 111 plane and linear methylethynyl is 90° .

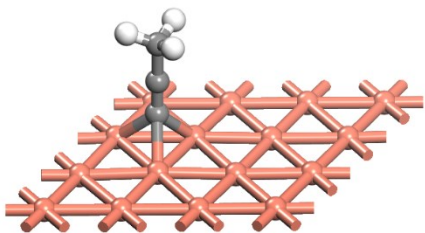
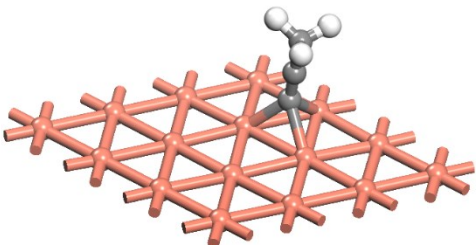
Sites	The optimized structures	BE (eV)
top	Relaxed to hcp	/
bridge	Relaxed to fcc	/
hcp		-4.23
fcc		<u>-4.24</u>

Table S4. The orientation, the optimized geometry structures and binding energies (per ligand) for $\text{CH}_3\text{C}\equiv\text{C}-\text{Au}_{\text{adatom}}-\text{C}\equiv\text{CCH}_3$ staple motif at the bridge sites on Au(111). Only the topmost surface layer is shown. Color legend: $\text{Au}_{\text{adatom}}$, red; other Au, yellow; C, grey; H, white.

The orientation	The optimized structures	BE (eV)
		-3.04
		-3.32
		-3.28
		-3.09
		-3.32
		<u>-3.44</u>

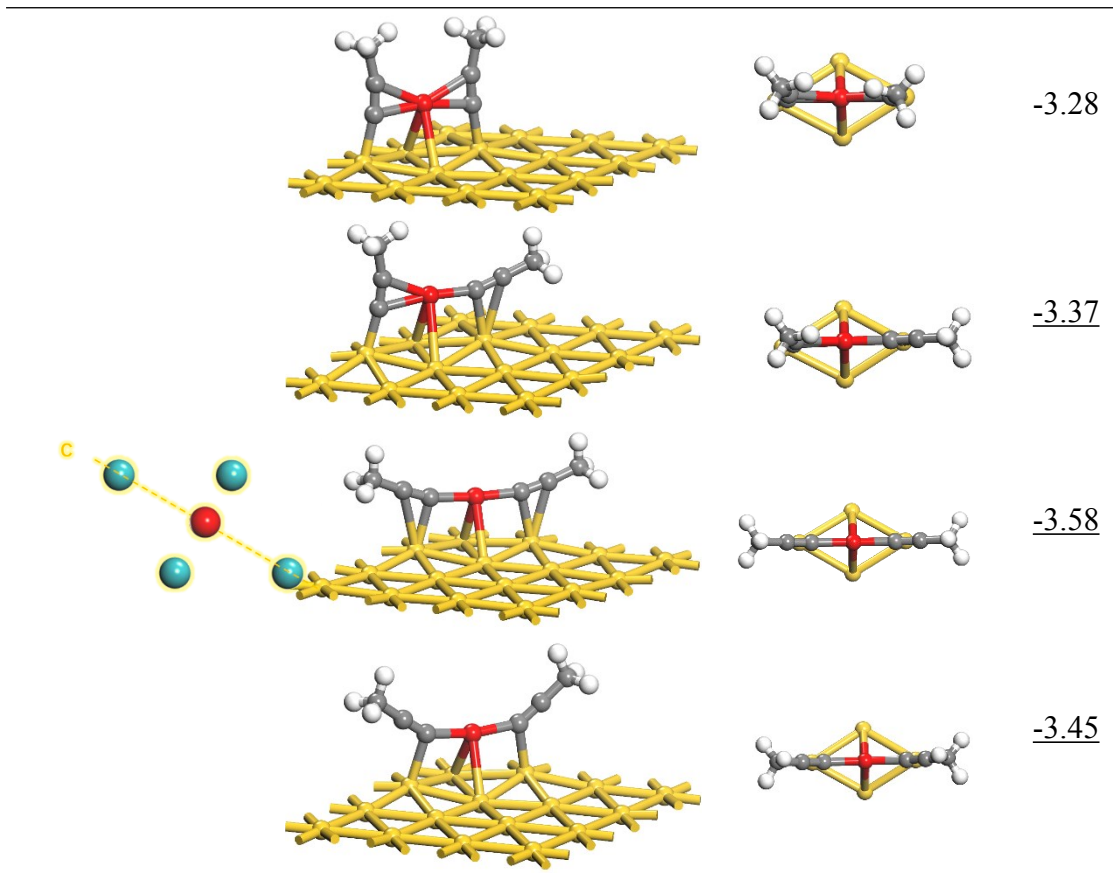
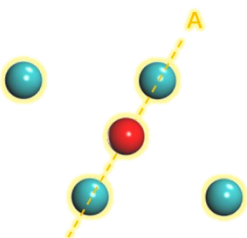
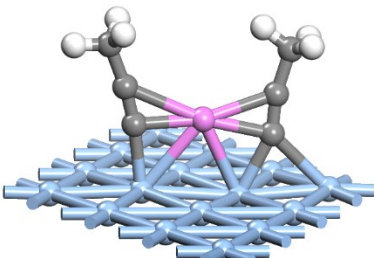
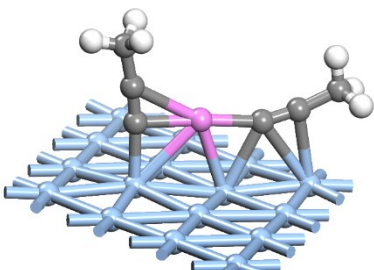
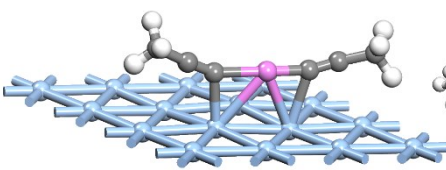
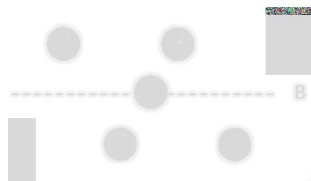
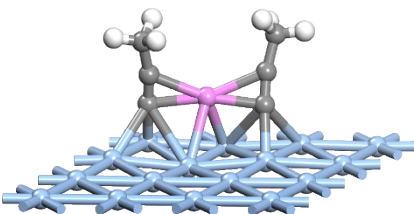
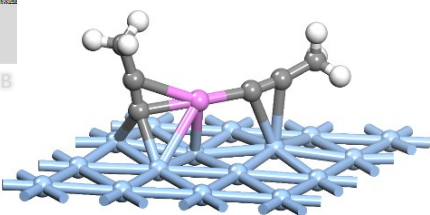
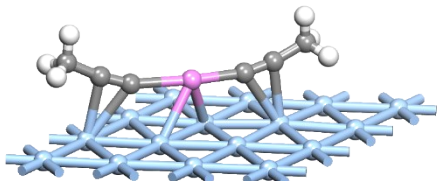
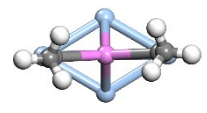
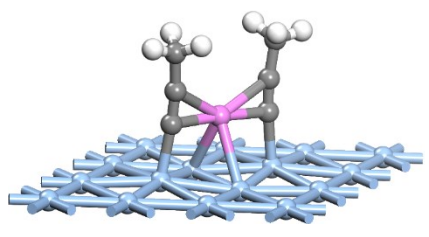
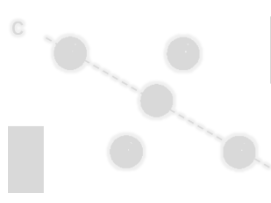
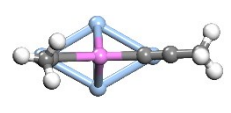
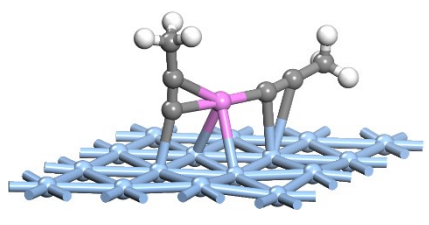


Table S5. The orientation, the optimized geometry structures and binding energies (per ligand) for $\text{CH}_3\text{C}\equiv\text{C}-\text{Ag}_{\text{adatom}}-\text{C}\equiv\text{CCH}_3$ staple motif at the bridge sites on Ag(111). Only the topmost surface layer is shown. Color legend: $\text{Ag}_{\text{adatom}}$, purple; other Ag, baby blue; C, grey; H, white.

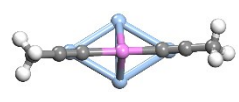
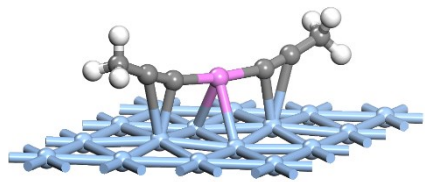
The orientation	The optimized structures	BE (eV)
		-3.16
		-3.31
		-3.35
		-3.22
		-3.41
		<u>-3.47</u>



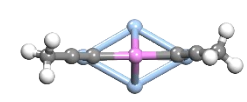
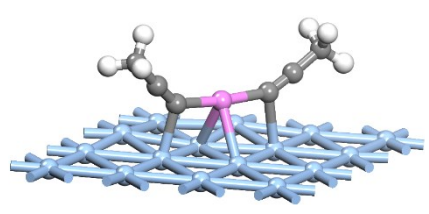
-3.23



-3.44

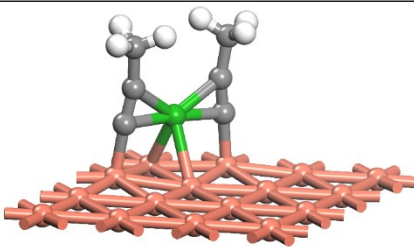
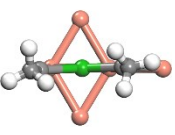
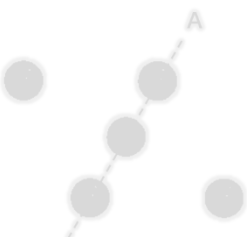
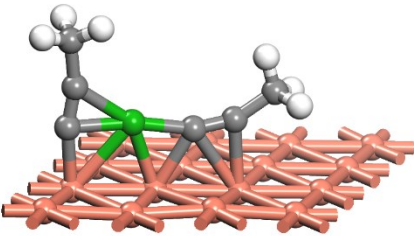
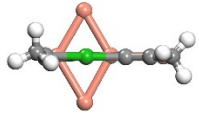
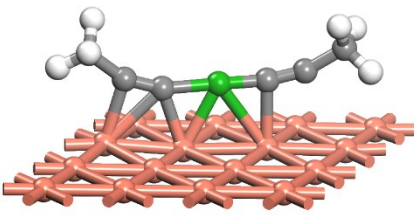
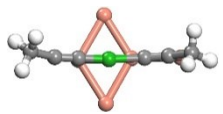
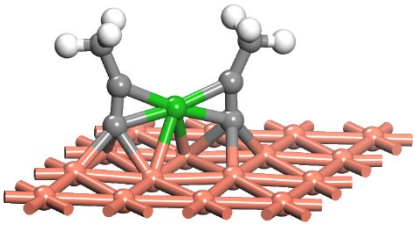
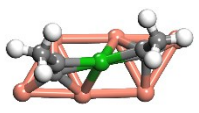
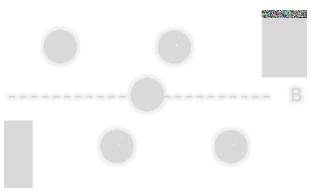
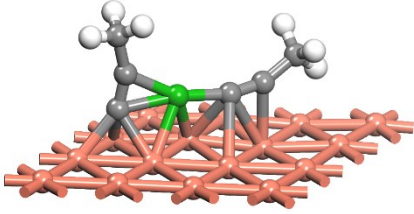
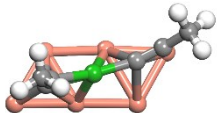
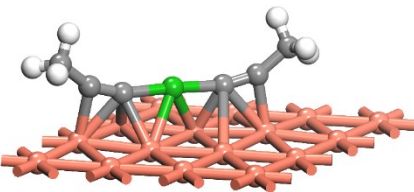
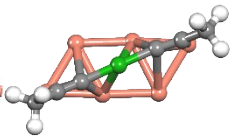


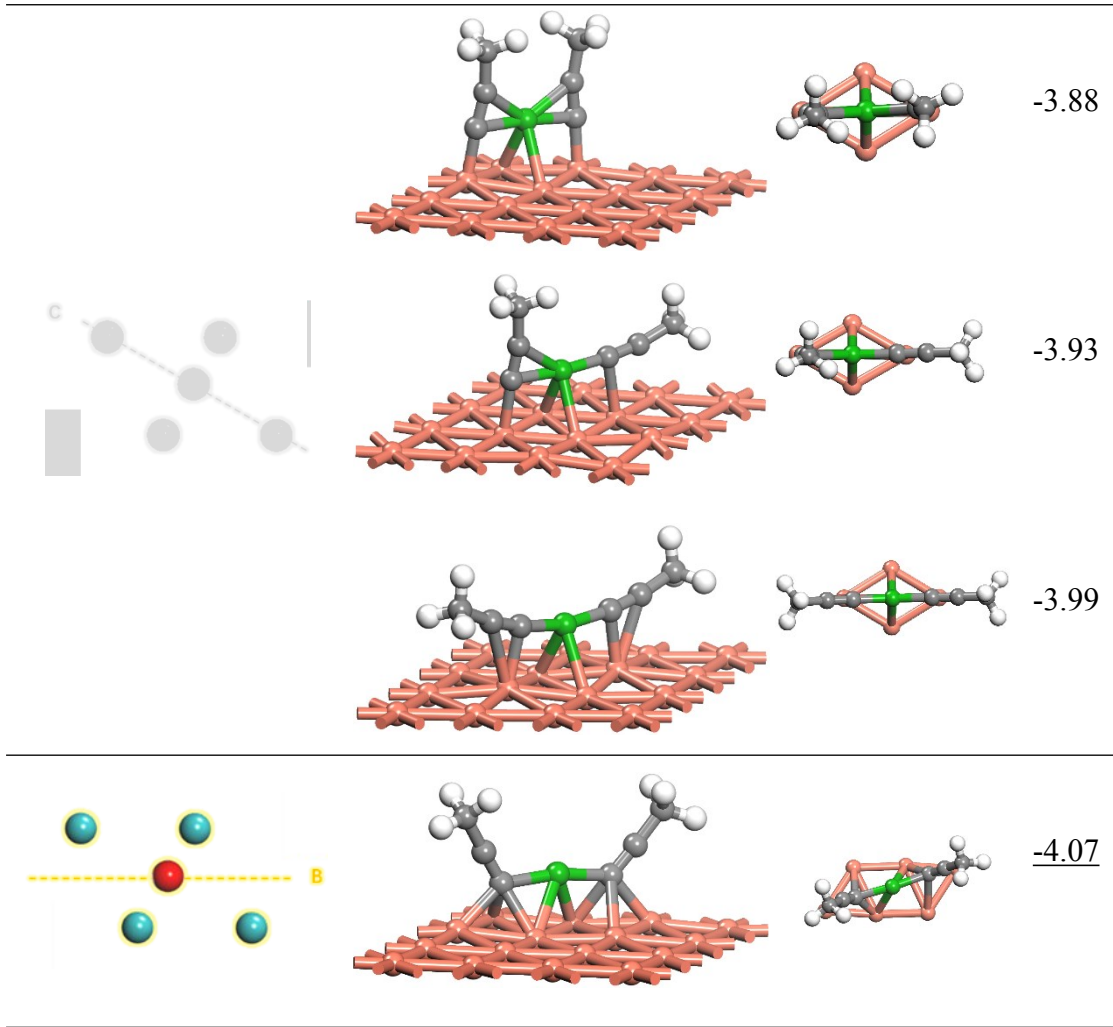
-3.48



-3.46

Table S6. The orientation, the optimized geometry structures and binding energies (per ligand) for $\text{CH}_3\text{C}\equiv\text{C}-\text{Cu}_{\text{adatom}}-\text{C}\equiv\text{CCH}_3$ staple motif at the bridge sites on $\text{Cu}(111)$. Only the topmost surface layer is shown. Color legend: $\text{Cu}_{\text{adatom}}$, green; other Cu, brick-red; C, grey; H, white.

The orientation	The optimized structures	BE (eV)
	 	-3.89
	 	-3.96
	 	-3.96
	 	<u>-4.14</u>
	 	<u>-4.13</u>
	 	<u>-4.12</u>



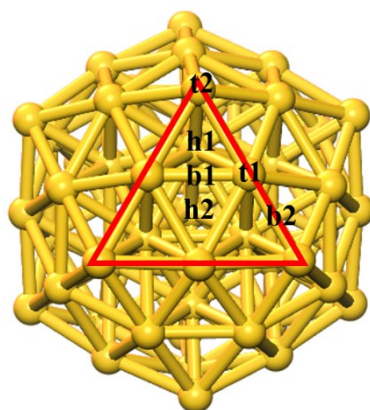


Figure S1. Schematic presentation of adsorption sites of high-symmetry on a triangular face of the Au₅₅ nanocluster.

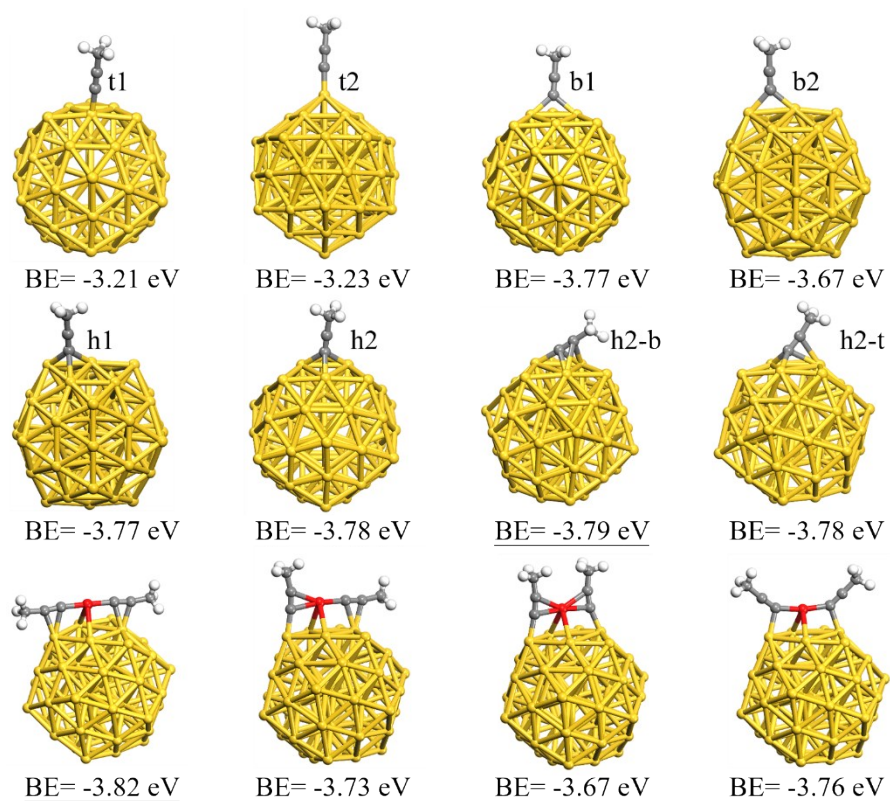


Figure S2. The binding energies and optimized structures of $\text{CH}_3\text{C}\equiv\text{C}$ covalently bonded to icosahedral Au_{55} cluster. Color legend: $\text{Au}_{\text{adatom}}$, red; other Au, yellow; C, grey; H, white.

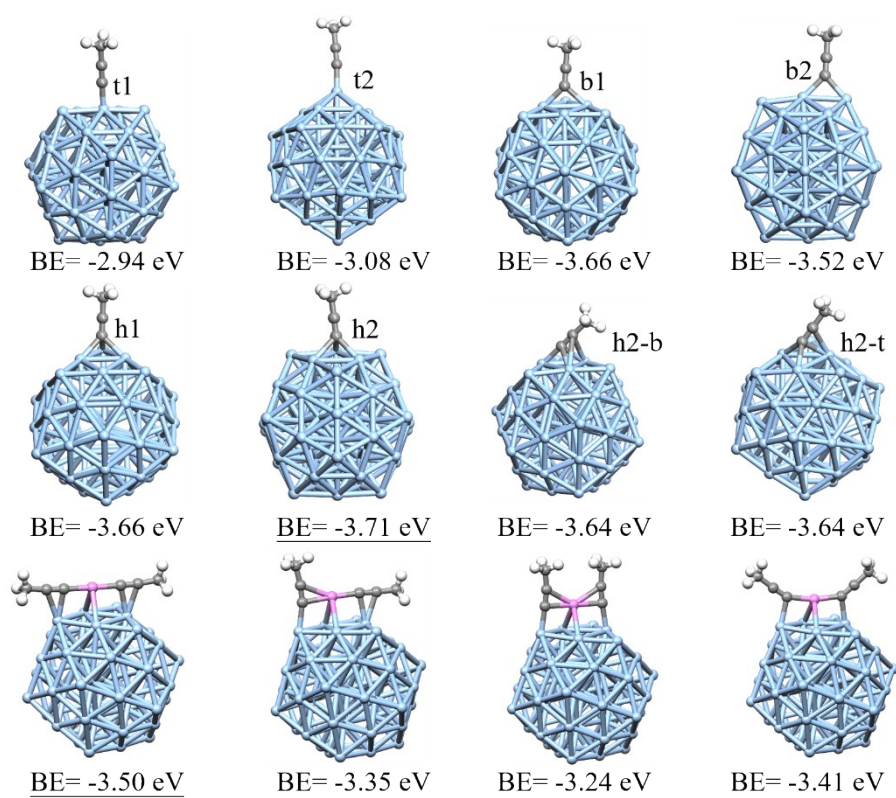


Figure S3. The binding energies and optimized structures of $\text{CH}_3\text{C}\equiv\text{C}$ covalently bonded to icosahedral Ag_{55} cluster. Color legend: $\text{Ag}_{\text{adatom}}$, purple; other Ag, baby blue; C, grey; H, white.

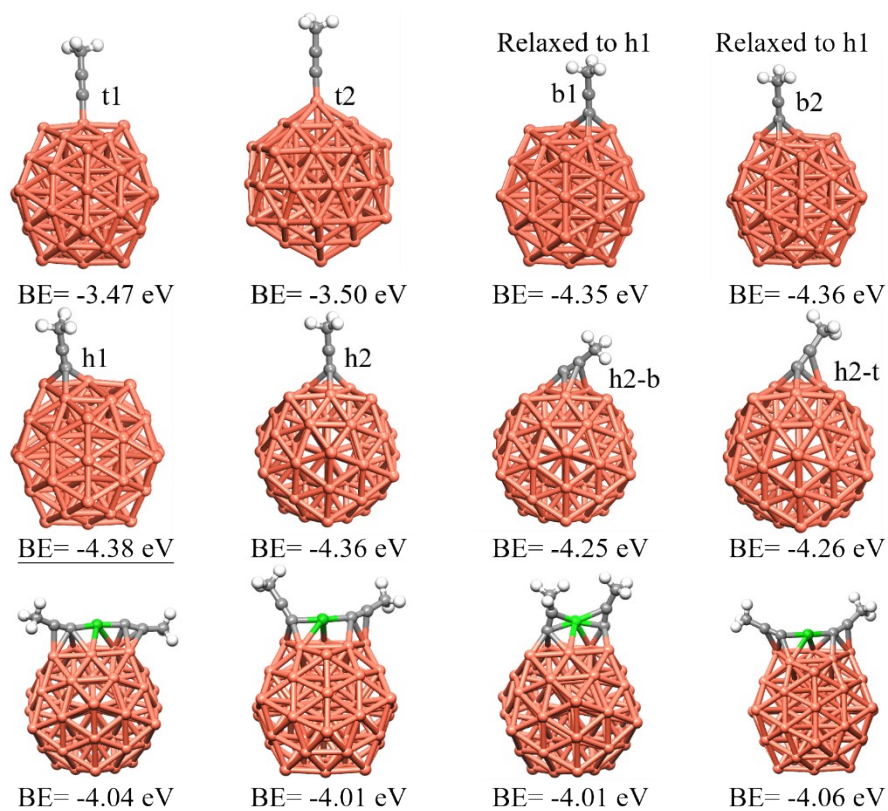


Figure S4. The binding energies and optimized structures of $\text{CH}_3\text{C}\equiv\text{C}$ covalently bonded to icosahedral Cu_{55} cluster. Color legend: $\text{Cu}_{\text{adatom}}$, green; other Cu, brick-red; C, grey; H, white.

Table S7. Comparison of binding energies per $\text{CH}_3\text{C}\equiv\text{C}$ - for the most stable mode of the bridge and staple motifs on the three coinage metal(111) surfaces with and without including the D3 approximation.

The most stable Mode		Category	PBE-D3 level	PBE (without vdW correction)
Au(111)	Bridge motif		-3.54 eV	-3.17 eV
	Staple motif		-3.58 eV	-2.87 eV
Ag(111)	Bridge motif		-3.55 eV	-3.29 eV
	Staple motif		-3.48 eV	-2.90 eV
Cu(111)	Bridge motif		-4.26 eV	-3.86 eV

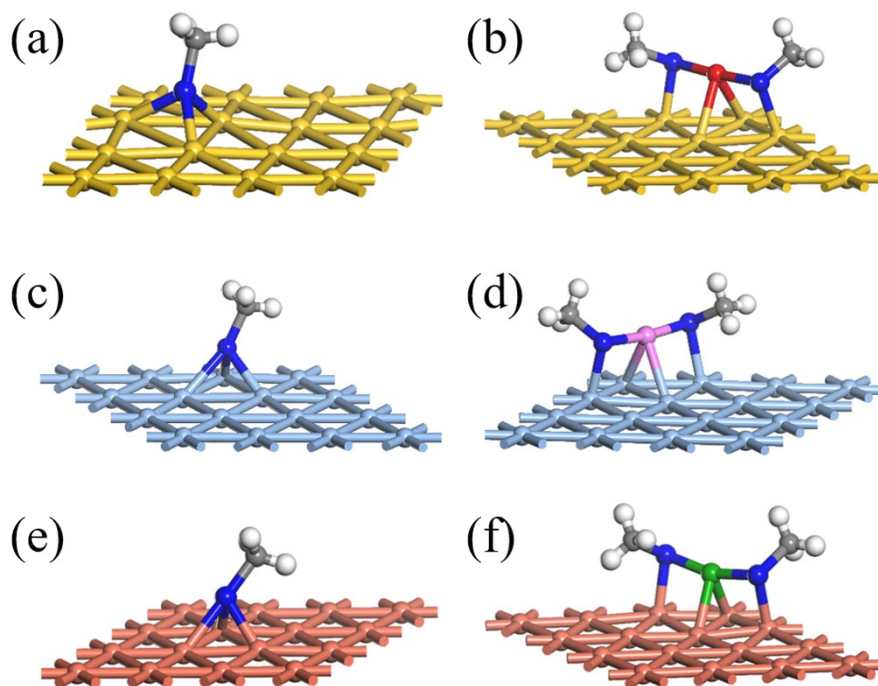


Figure S5. The optimized structures (only the topmost surface layer is shown) of methylthiolate (CH_3S^-) for the bridging and staple motifs on (a-b) Au(111), (c-d) Ag(111), and (e-f) Cu(111) with 4 layers of slab in a 4×4 lateral cell. The initial angle between the surface normal and S-C bond is 30° . S atom is highlighted in blue.